Isotopic Exchange of Oxygen between Proton-Exchanged Zeolites and Water

Noritaka Mizuno,*,† Hiroshi Mori,‡ Kazue Mineo, and Masakazu Iwamoto*

Catalysis Research Center, Hokkaido University, Sapporo 060-0811, Japan

Received: July 1, 1999; In Final Form: September 15, 1999

The time courses of the title reaction were analyzed by using a closed circulation system. It was found that there are three kinds of framework oxygen, O_I, O_{II}, and O_{III}, that is, easily, moderately, and hardly exchanging oxygens. The respective rate constants of the exchange reaction, k_1, k_2, and k_3, were almost constant, or independent of the zeolite structures and silica/alumina ratios. In contrast, the numbers of O_I and O_{II} (n_1 and n_2) decreased with increasing silica/alumina ratios, whereas that of O_{III} (n_3) increased. $n_1 + n_2$ and n_3 are approximately in agreement with the numbers of bridging oxygens of Si−O−Al and Si−O−Si, respectively. Next, IR measurement was applied to confirm the origin of the active framework oxygens. Upon the exchange reaction on H-MFI-23, one acidic OH band at 3612 cm^{-1} readily shifted to lower frequency while the silanol band at 3735 cm^{-1} and ν(Si−O−T (T = Si or Al)) bands at 1219 and 1092 cm^{-1} shifted slightly. The ^{18}O contents in the bands, evaluated by the deconvolution of the spectra, decreased in the following order: acidic OH ≫ Si−O−T = silanol. A similar order was observed on H-FAU-5.6, H-MOR-16, or H-LTL-6.0. Most of oxygens corresponding to the acidic OH bands could exchange with ^{18}O upon treatments in a large excess of $H_2{}^{18}O$. It follows that O_I and O_{II} are the bridging oxygens bound to Al and exchangeable with water by the contribution of neighboring proton, and O_{III} is the bridging oxygen between two Si atoms. It was further found that the exchange reaction, Si−^{18}O−Al + Si−^{16}O−Si → Si−^{16}O−Al + Si−^{18}O−Si, starts to proceed above 673 K and is dominant at 873 K.

Introduction

Zeolites are crystalline aluminosilicates having a channel or cage structure. Various kinds of zeolites and related microporous oxides with various compositions and pore sizes have been reported.[1−4] Zeolites can catalyze selective reactions[5−11] and can do selective adsorptions.[12] Recently, the acidic sites have been characterized by solid-state NMR and IR spectroscopy[13−19] and theoretical simulations in relation to the catalysis.[20,21] Metal ions incorporated into the zeolite framework have also been widely investigated as well as Si and Al ions. However, very little is known of the properties of framework oxygens, which are the surface atoms of zeolite cages and which can stabilize the reaction intermediates and metal cations.[20−23] Framework oxygens of zeolites can be exchanged with those of H_2O, CO_2, O_2, and NO while keeping their highly crystalline frameworks.[24−29] Oxygen is included in many kinds of reactions such as oxidation, hydration, and formation of aluminosilicate anions to give the zeolites.[2,30] It is highly significant to know the characteristics of the framework oxygen toward the exchange reaction, because they are indispensable for elucidation of the true mechanisms of oxygen-containing reactions. In particular, the investigation of oxygen exchange between zeolites and water molecules is important to understand the formation of zeolite structure and catalysis on the surface.

The oxygen exchange between Y-type or ZSM-5 zeolites and water has been phenomenologically reported first by one of the present authors[24] and then by Ballmoos and Meier.[25] However, little is known of the active sites for and the reaction mechanism of the exchange. We have preliminarily reported for proton-exchanged ZSM-5 zeolites that there are three kinds of framework oxygens: O_I, O_{II}, and O_{III}, corresponding to easily, moderately, and hardly exchanging oxygens, respectively.[24] Recently, Xu and Stebbins have also reported that there are two kinds of framework oxygens for sodium and calcium ion-exchanged natural stilbite.[31]

In the present work, we studied the oxygen exchange between water molecules and zeolites having various structures and a range of silica/alumina ratio of 5.6−50, clarified the positions of O_I, O_{II}, and O_{III}, and attempted to reveal the exchange mechanism.

Experimental Section

Materials and Characterization. Parent zeolites, ZSM-5 (denoted as MFI) with silica/alumina ratio of 23, 40, and 50, ferrierite (FER, 12 and 17), L-type (LTL, 6.0), mordenite (MOR, 11, 15, and 19), and Y-type (FAU, 5.6) zeolites were supplied by Tosoh Corp.

Each proton-exchanged zeolite was prepared as follows.[29] Approximately 20 g of each zeolite was washed in 2 dm^3 of dilute $NaNO_3$ solution and then ion-exchanged in 1 dm^3 of NH_4NO_3 solution of 0.25 mol dm^{-3} overnight. After filtration, the resulting cake was washed and dried for ca. 12 h at 343−383 K and the resultant $NH_4{}^+$-zeolite was calcined at 773−813 K for 2−4 h. The exchange level of proton in each zeolite was approximately 100%, which was confirmed by the amounts of residual Na^+ or K^+ ion on zeolites. The zeolites obtained were abbreviated as for example H-MFI-23 (cation-zeolite structure-silica/alumina ratio).

The amounts of Al, Si, and Na or K in each zeolite were determined by atomic absorption spectroscopy after each zeolite

* To whom correspondence should be addressed.

† Present address: Department of Applied Chemistry, Graduate School of Engineering, The University of Tokyo, Hongo, Bunkyo-ku, Tokyo 113-8656, Japan.

‡ Present address: Department of Industrial Chemistry, Miyakonojo College of Technology, Miyakonojo 885-0004, Miyazaki, Japan.

10.1021/jp992258l CCC: $18.00
Published on Web 11/05/1999

TABLE 1: Chemical Composition of Zeolites Used and Number of Framework Oxygens

					no. of framework oxygens/mmol g^{-1}	
no.	catalyst	chemical composition[a]	no. of Al/mmol g^{-1}	SiO_2/Al_2O_3 ratio[a]	Si−O−Al[b]	Si−O−Si
1	H-MFI-23	$H_{7.5}Na_{0.1}Al_{7.6}Si_{88.4}O_{192}\cdot 16H_2O$	1.32	23.3	5.3	28.0
2	H-MFI-40	$H_{4.5}Al_{4.5}Si_{91.5}O_{192}\cdot 16H_2O$	0.78	40.4	3.1	30.2
3	H-MFI-50	$H_{3.7}Al_{3.7}Si_{92.3}O_{192}\cdot 16H_2O$	0.64	49.8	2.6	30.7
4	H-FER-12	$H_{5.0}Al_{5.0}Si_{31.0}O_{72}\cdot 18H_2O$	2.32	12.4	9.3	24.0
5	H-FER-17	$H_{3.6}K_{0.2}Al_{3.8}Si_{32.2}O_{72}\cdot 18H_2O$	1.76	16.8	7.0	26.3
6	H-MOR-11	$H_{7.7}Al_{7.7}Si_{40.3}O_{96}\cdot 24H_2O$	2.67	10.5	10.7	22.6
7	H-MOR-15	$H_{5.5}Na_{0.1}Al_{5.6}Si_{42.4}O_{96}\cdot 24H_2O$	1.94	15.0	7.8	25.5
8	H-MOR-19	$H_{4.6}Al_{4.6}Si_{43.4}O_{96}\cdot 24H_2O$	1.60	18.9	6.4	26.9
9	H-LTL-6.0	$H_{8.5}K_{0.5}Al_{9.0}Si_{27.0}O_{72}\cdot 22H_2O$	4.17	6.0	16.7	16.6
10	H-FAU-5.6	$H_{50.5}Al_{50.5}Si_{141.5}O_{384}\cdot 250H_2O$	4.38	5.6	17.5	15.8
11	Na-FAU-5.6	$Na_{50.5}Al_{50.5}Si_{141.5}O_{384}\cdot 250H_2O$	4.38	5.6	17.5	15.8

[a] Determined by atomic absorption spectroscopy. [b] 4 × number of Al, including that of acidic OH groups.

TABLE 2: Number of Al and Framework Oxygens Determined by ^{29}Si NMR Analysis

		no. of framework oxygens[a]/mmol g^{-1}			
zeolite	SiO_2/Al_2O_3 ratio	Si(0Al)−O−Si	Si(1Al)−O−Al	Si(2Al)−O−Al	Si(3Al)−O−Al
H-MFI-23	25.0	28.4	3.2	1.7	0
H-MFI-40	40.7	30.2	3.1	0	0
H-MFI-50	51.2	30.8	2.5	0	0
H-MOR-11	11.4	23.4	7.0	2.9	0
H-MOR-15	15.6	25.8	6.3	1.2	0
H-MOR-19	19.0	27.0	5.7	0.6	0
H-LTL-6.0	6.6	17.0	6.4	6.9	3.0
H−FAU-5.6	5.4	15.5	4.9	10.2	2.7

[a] Si with zero, one, two, and three Al nearest neighbors are designated by Si(0Al), Si(1Al), Si(2Al), and Si(3Al), respectively.

sample was dissolved in a hydrogen fluoride solution. The silica/alumina ratios in the zeolite framework were also determined by ^{29}Si MAS NMR (Bruker AC 300) as described previously.[32] The chemical compositions and numbers of framework oxygen are summarized in Tables 1 and 2. The numbers of bridging framework oxygens of Si−O−Al and Si−O−Si were calculated by 4 × (number of Al atoms) and (total amount of the framework oxygen) − 4 × (number of Al atoms), respectively. The SiO_2/Al_2O_3 ratios obtained by atomic absorption spectroscopy well agreed with those obtained by ^{29}Si MAS NMR as shown in Tables 1 and 2, indicating that there is no extraframework aluminum ion on these zeolites and that the dealumination occurred during the preparation. It is assumed that the number of acidic OH is equal to that of Al atoms in zeolites and is included in the number of Si−O−Al mentioned above.

$NaNO_3$ and NH_4NO_3 were reagent grade and used without further purification.

Powder X-ray diffraction patterns were recorded on a powder X-ray diffractometer (MAC Science, MXP^3) by using Cu Kα radiation. It was confirmed for H-MFI-23 and H-MOR-15 that the XRD patterns were not changed by the following ^{18}O-exchange experiments with $H_2{}^{18}O$ at 573 K.

Exchange Reaction. The exchange reaction was carried out in a closed circulation system of 196 cm^3 at 423−873 K at the pressure of $H_2{}^{18}O$ (99%), 0.5−2.3 kPa (standard, 1.7 kPa), using ca. 12−20 mg zeolites. The isotopic distribution of oxygen in water was measured by a mass spectrometer. The standard pretreatment was as follows: the sample was heated at 873 K under vacuum, evacuated for 30 min, exposed to O_2 (39.9 kPa), evacuated again for 30 min, and then cooled to a reaction temperature. This was performed to remove such impurities on the zeolite surface as water, carbon dioxide, and oxygen.

IR Spectra. IR spectra were measured as follows: A self-supporting zeolite wafer (11−13 mg, 1.2−1.7 cm^2) was prepared by pressing powder zeolites under the pressure of 200 kg cm^{-2} for 30 min. The wafer was placed in a quartz infrared cell with KBr windows directly connected to the circulation system as described previously.[33] The exchange reaction on the wafer was carried out in the same way as that described for the powder zeolite. After the reaction was carried out for a prescribed period, the wafer was evacuated at the reaction temperature for 30 min and cooled to room temperature, and then the IR spectrum in the range 3000−4000 cm^{-1} was measured. Since ν(Si−O−T) bands were much more intense than ν(OH) bands, absorbances of the ν(Si−O−T) bands were saturated. Therefore, the IR spectra in the range 800−1500 cm^{-1} were measured by exposing the wafer to dry nitrogen and pressing it with KBr under N_2. All IR spectra were measured at 1 cm^{-1} resolution with FTS-7 (Bio-rad) or Paragon 1000PC (Perkin-Elmer) spectrometer and room temperature. It is assumed that the absorption coefficient of ν(Si−O−Al) is equal to that of ν(Si−O−Si).

Results and Discussion

Kinetics of Exchange. The ^{18}O content in the gas phase water on proton-exchanged zeolites with different structures and silica/alumina ratios are shown as a function of the reaction time in Figure 1, a and b, respectively. Initially, the ^{18}O content in gas phase water decreased steeply, then gradually decreased, and finally reached an approximately constant value. Similar time courses were observed on all of the zeolites used. The initial dramatic decrease in the ^{18}O content shows the existence of the easily exchangeable framework oxygen. The almost constant values after ca. 300 min suggest that a portion of framework oxygen can hardly take part in the exchange at 573 K. The amount of water uptake for each zeolite upon the introduction of water vapor was less than 2% of that of the water introduced. It was confirmed in a separate temperature-programmed desorption experiment that the amount of water desorbed in the range 873−1273 K was less than one-half of that desorbed in the range 573−873 K. These facts show that the amount of water adsorbed on the zeolite under the reaction conditions was less than 0.1 of the number of water molecule per Al site in

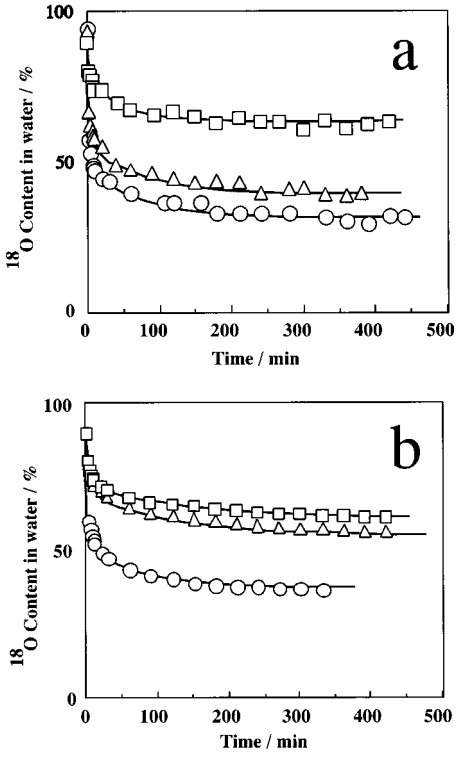

Figure 1. Time courses of ^{18}O contents in gas-phase water at 573 K. Sample weight, 20 mg; P_{H_2O}, ca. 1.7 kPa. (a) (□) H-MFI-50; (△) H−FAU-5.6; (○) H-MOR-11; (■) calculated line. (b) (□) H-MFI-50; (△) H-MFI-40; (○) H-MFI-23; (−) calculated line.

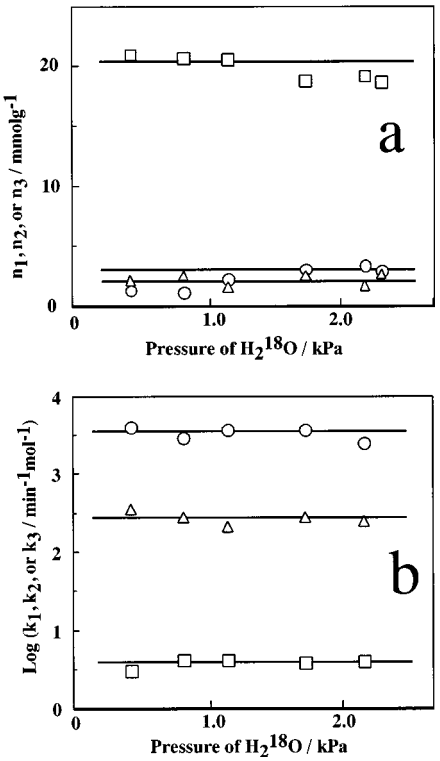

Figure 2. Dependence of n_1, n_2, and n_3 (a) or k_1, k_2, and k_3 (b) on partial pressure of $H_2{}^{18}O$. Sample, H-FAU-5.6; reaction temperature, 573 K. (a) (○) n_1; (△) n_2; (□) n_3. (b) (○) k_1; (△) k_2; (□) k_3.

zeolite and negligible in comparison with that of gas phase water, and exclude the possibility that the observed oxygen exchange might be due to exchange between water taken up and water still remained in the zeolite framework.

The decrease in the ^{18}O content is simulated by the following equation, which has been applied by Takaishi and Endoh[27] and Yashima et al.[28]

$$n_g \, dy_g/dt = -n_g y_g \sum k_i n_i (1 - y_i) + n_g (1 - y_g) \sum k_i n_i y_i \qquad (1)$$

where the subscript g designates the gas phase water, there are j kinds of framework oxygen, n and k are the number of oxygen atoms in each oxygen phase and the rate constant of exchange, respectively, and y is the fraction of ^{18}O. In the simulation, $n_1 + n_2 + \cdots + n_j$ corresponds to the total oxide ion in zeolite framework. n_i and k_i are estimated by Runge−Kutta method. As shown by the solid line in Figure 1a,b, the change in the ^{18}O content was well reproduced on the assumption that there are three kinds of framework oxygen, O_I, O_{II}, and O_{III}, which correspond to easily, moderately, and hardly exchanging oxygens, respectively. The experimental data could not be reproduced by using one or two kinds of framework oxygen. Therefore, zeolites have at least three kinds of framework oxygens exchangeable with water molecules.

The values of n_i and k_i ($i = 1-3$) of H-MFI-23 and H-FAU-5.6 were almost constant at 573 K in the range of the partial pressure of water vapor 0.5−2.3 kPa. The results for FAU-5.6 are shown in Figures 2a,b as an example. These data show that the rate-limiting step is not the diffusion of water vapor into zeolite micropores.

The values of n_1, n_2, n_3, k_1, k_2, and k_3 for proton-exchanged zeolites obtained by the simulation are listed in Table 3. The values of k_1, k_2, and k_3 were 5750 ± 1250, 240 ± 60, and 2.8 ± 2.2, respectively, but were not correlated with zeolite

TABLE 3: Parameters of Eq 1, n_1, n_2, n_3, k_1, k_2, and k_3, Calculated for Zeolite[a]

	n/mmol g^{-1}			k/min^{-1} mol^{-1}		
zeolite	n_1	n_2	n_3	k_1	k_2	k_3
H-MFI-23	3.00	3.33	27.0	7000	200	1.1
H-MFI-40	1.13	1.33	30.8	5500	240	0.9
H-MFI-50	1.00	1.10	31.2	5500	240	0.6
H-FER-12	5.00	2.50	25.8	5000	250	2.6
H-FER-17	3.90	4.00	25.4	4600	280	2.6
H-MOR-11	5.66	4.33	23.3	5000	180	4.0
H-MOR-15	5.83	4.33	23.1	5000	230	4.0
H-MOR-19	4.10	3.56	25.6	6000	240	2.5
H-LTL-6.0	4.66	5.33	23.3	6700	300	5.0
H-FAU-5.6	4.06	3.43	25.8	4500	280	4.0
Na-FAU-5.6[b]	*c*	0.76	29.6	*c*	170	0.7

[a] Reaction temperature 573 K. [b] The exchange level of Na^+, 100%. [c] No easily exchanged oxygen was observed.

structures and silica/alumina ratios. In contrast, n_1, n_2, and n_3 changed with the change in ratios.

The changes in n_1, n_2, and n_3 for H-MFI-23 with reaction temperatures are shown in Figure 3a. The values were almost constant below 573 K. Above 673 K, n_3 gradually decreased and much decreased at 873 K while n_1 and n_2 increased. This is due to the ^{18}O exchange of Si−^{18}O−Al with Si−^{16}O−Si in addition to that of $H_2{}^{18}O$ with Si−^{16}O−Al as discussed in the later part. Therefore, the activation energies of k_1, k_2, and k_3 were calculated for the data below 573 K. Approximately linear correlations of the Arrhenius plots for k_1, k_2, and k_3 gave the activation energies, 8, 8, and 18 kJ/mol, respectively.

Figure 4 shows the correlations between $n_1 + n_2$ and the number of bridging oxygen of Si−O−Al and between n_3 and the number of bridging oxygen of Si−O−Si. It is noted that $n_1 + n_2$ and n_3 are approximately in agreement with the numbers of bridging oxygens of Si−O−Al and Si−O−Si, respectively. The findings will be discussed later with the IR measurements,

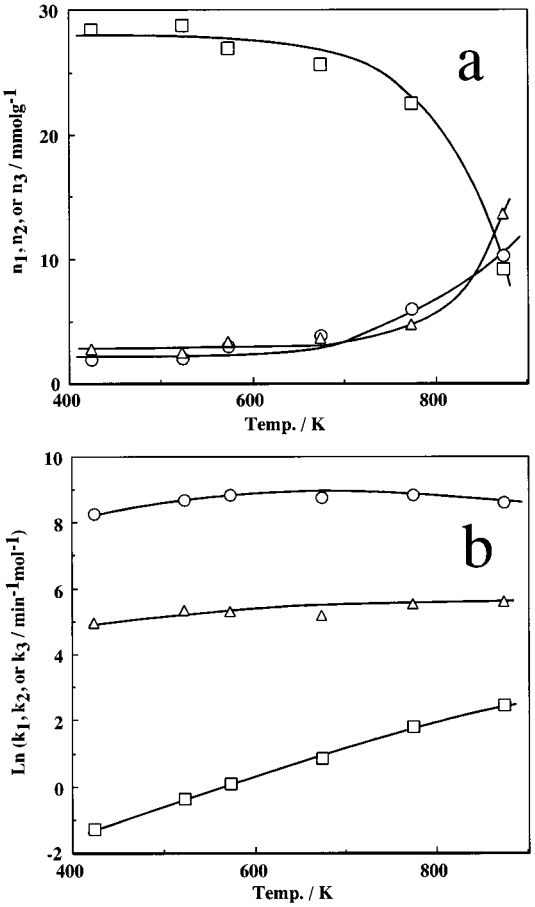

Figure 3. Changes in n_1, n_2, and n_3 (a) or k_1, k_2, and k_3 (b) for H-MFI-23 with reaction temperatures. Symbols, the same as those in Figure 2.

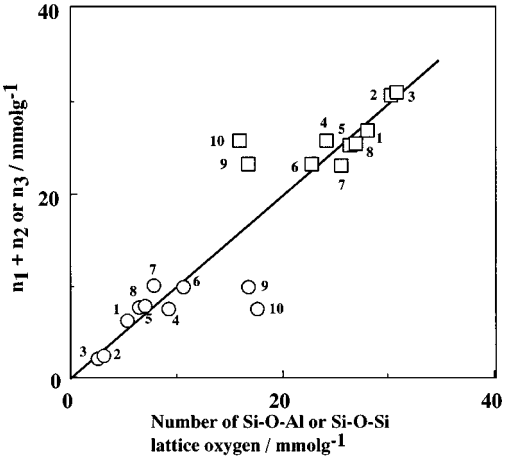

Figure 4. Correlations between $n_1 + n_2$ and the number of Si−O−Al oxide ions or n_3 and number of Si−O−Si framework oxygens. Reaction temperature, 573 K. (○) Correlation between $n_1 + n_2$ and number of Si−O−Al framework oxygen; (□) correlation between $n_1 + n_2$ and n_3 and number of Si−O−Si framework oxygen. For the sample numbers attached, see Table 1.

but it should be noted that the data of H-FAU-5.6 and H-LTL-6.0 deviated from the line. Among the zeolites tested, these two zeolites have lower SiO_2/Al_2O_3 ratios and Si(3Al)−O−Al bridging framework oxygens as shown in Table 2. The deviation may result from slow ^{18}O exchange of Si(3Al)−O−Al with water. The lower activities per Al atoms in the high-alumina content zeolites have indeed been reported for several catalytic reactions.[16] The proper reason should be clarified in the future.

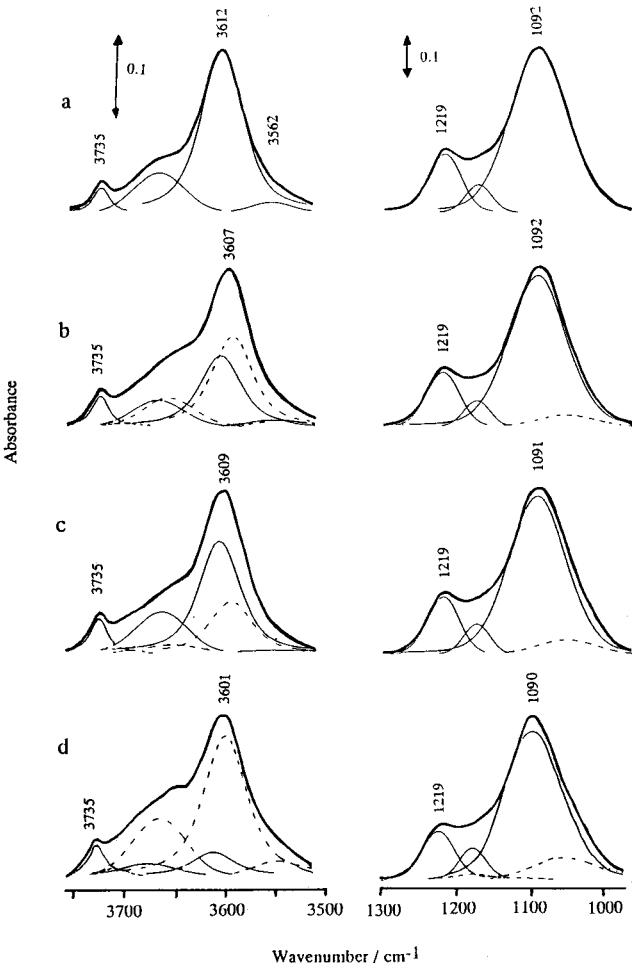

Figure 5. Changes in IR spectra of H-MFI-23 with various treatments: (a) before ^{18}O exchange with $H_2{}^{18}O$ vapor; H-MFI-23 was kept in contact with $H_2{}^{16}O$ (1.7 kPa) at 573 K for 3 h followed by the evacuation at the same temperature for 0.5 h; (b) after ^{18}O exchange with $H_2{}^{18}O$ vapor (1.7 kPa) at 573 K for 2 h followed by the evacuation at the same temperature for 30 min; (c) after the successive evacuation of (b) at 873 K for 1 h; (d) after ^{18}O exchange with a large excess of $H_2{}^{18}O$ at 573 K for 5 h followed by the evacuation at the same temperature for 30 min. (—) IR bands assignable to the species containing ^{16}O; (− − −) those of ^{18}O. The ^{16}OH and Si−^{16}O−T regions of H-MFI-23 were deconvoluted into four (3735 (3723), 3676 (3664), 3612 (3600), and 3562 (3550) cm^{-1}; numbers in parentheses are corresponding ^{18}OH band positions) and three (1219 (1175), 1174 (1132), and 1092 (1053) cm^{-1}; numbers in parentheses are corresponding Si−^{18}O−T band positions) bands, respectively, because the IR spectra could not be well reproduced by using fewer bands. However, this would not affect the later discussion since ^{18}O content of acidic OH was calculated by the sum of the three band areas.

IR Spectra and Exchange Mechanism. IR spectra of H-MFI-23 are shown in Figure 5. As shown in Figure 5a, H-MFI-23 showed the bands at 3735, 3612, 1219, and 1092 cm^{-1} in ν(OH) and ν(Si−O−T (T = Si, Al)) regions when it was kept in contact with $H_2{}^{16}O$ (1.7 kPa) at 573 K for 3 h followed by the evacuation at the same temperature for 30 min. In comparison with literature values,[34−39] each band can be assigned as follows: 3735 cm^{-1}, ν(silanol); 3612 cm^{-1}, ν(acidic OH); 1219 and 1092 cm^{-1}, ν(Si−O−T). The spectrum changed to Figure 5b upon contact with $H_2{}^{18}O$ (1.7 kPa) at 573 K for 2 h and the evacuation at the same temperature for 30 min. The 3735, 1219, and 1092 cm^{-1} bands little shifted, showing the slow isotopic exchange of oxygen between water and SiOH or Si−O−T. On the other hand, the band at 3612 cm^{-1} shifted to 3607 cm^{-1}, demonstrating the fast exchange.

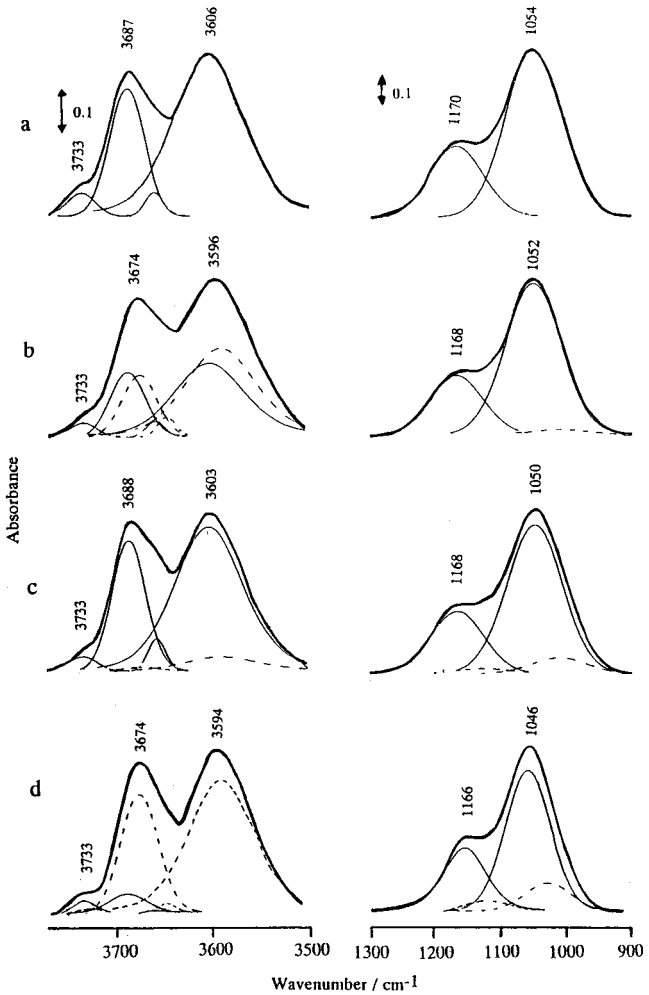

Figure 6. Changes in IR spectra of H−FAU-5.6 with various treatments: (a) before ^{18}O exchange with $H_2{}^{18}O$ vapor; H-FAU-5.6 was kept in contact with $H_2{}^{16}O$ (1.7 kPa) at 573 K for 3 h followed by the evacuation at the same temperature for 30 min; (b) after ^{18}O exchange with $H_2{}^{18}O$ vapor (1.7 kPa) at 573 K for 2 h followed by the evacuation at the same temperature for 30 min; (c) after the succesive evacuation of (b) at 873 K for 1 h; (d) after ^{18}O exchange with a large excess of $H_2{}^{18}O$ at 573 K for 3 h followed by the evacuation at the same temperature for 30 min. (−) IR bands assignable to the species containing ^{16}O; (− − −) those of ^{18}O. The ^{16}OH and Si−^{16}O−T regions of H-FAU-5.6 were deconvoluted into four (3733 (3721), 3687 (3675), 3660 (3650), and 3606 (3594) cm^{-1}; numbers in parentheses are corresponding ^{18}OH band positions) and two (1170 (1128) and 1054 (1016) cm^{-1}; numbers in parentheses are corresponding Si-^{18}O−T band positions) bands, respectively. See note in Figure 5.

Similar results were obtained on H-FAU-5.6. IR spectra of H-FAU-5.6 showed the bands at 3733, 3687, 3606, 1170, and 1054 cm^{-1} in ν(OH) and ν(Si−O−T) regions when it was kept in contact with $H_2{}^{16}O$ (1.7 kPa) at 573 K for 3 h followed by the evacuation at the same temperature for 0.5 h (Figure 6a). Each band can be assigned as follows: 3733, ν(silanol); 3687 and 3606, ν(acidic OH); 1170 and 1054 cm^{-1}, ν(Si−O−T). As shown in Figure 6b, the spectrum varied when it was kept in contact with $H_2{}^{18}O$ (17 kPa) at 573 K for 2 h and the evacuation at the same temperature for 30 min. The ν(silanol) band hardly shifted, while the bands at 3687, 3606, 1170, and 1054 cm^{-1} clearly shifted to the respective lower frequencies.

The changes of ^{18}O contents in the bands for H-MFI-23 and H−FAU-5.6 are shown in Figure 7, a and b, respectively. In both figures, the ^{18}O contents in acidic OH sharply increased and reached almost constant values within ca. 10 min which were equal to the final values of gas phase water vapor whereas

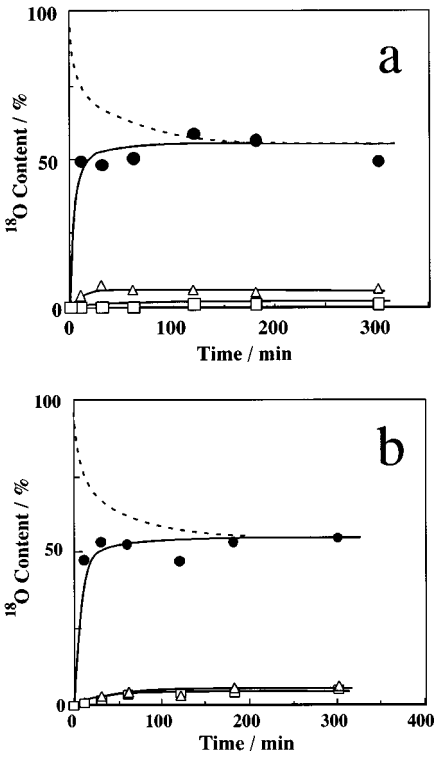

Figure 7. Time courses of ^{18}O contents in IR bands at 573 K. ●, □, △, − − − correspond to ^{18}O contents in the IR bands of acidic OH, Si−O−T, SiOH, and the gas-phase water, respectively. (a) Sample, H-MFI-23; (b) sample, H-FAU-5.6.

those of silanol and Si−O−T increased a little. The ^{18}O contents decreased in the order of acidic OH ≫ Si−O−T = silanol. The same orders were observed for H-MOR-16 and H-LTL-6.0.

Figures 5d and 6d show the spectra after the exchange treatment was carried out in a large excess of $H_2$18O at 573 K. The number of water molecules is ca. 10 times larger than the total numbers of framework oxygen in zeolite. The ^{18}O contents in the gas-phase water and the bands of acidic OH and Si−O−T after 5 h were 93, 92 (1.2 mmol g^{-1}), and 9.6% (3.1 mmol g^{-1}), respectively, as summarized in Table 4. Therefore, the total number of ^{18}O in H-MFI-23 was 4.3 mmol g^{-1}. This indicates that the number of active oxygens for the exchange at 573 K is about 4.7 mmol g^{-1} (=4.3/0.93). The value is approximately equal to that of Si−O−Al framework oxygen in H-MFI-23 (5.3 mmol g^{-1}, see Table 1) and that of $n_1 + n_2$ (6.33 mmol g^{-1}, see Table 3). These correspondences result in the expected consistency of the amount of unreactive ^{16}O (inactive for the exchange, 28.6 mmol g^{-1}) with that of n_3 (27 mmol g^{-1}). The same phenomena were observed on H-MOR-15.

To assign the O_I, O_{II}, and O_{III} species we have the following findings. (1) The $n_1 + n_2$ and n_3 values are in fair agreement with the amounts of $O_I + O_{II}$ and O_{III}, respectively, as shown in Figure 4. (2) The n_1 values are approximately equal to the n_2 values for the respective samples (Table 3), regardless of the zeolite structures and aluminum contents. (3) The acidic OH groups could be easily exchanged at 573 K, while most of Si−O−T remained unchanged. (4) Upon treatment in a large excess of $H_2{}^{18}O$ at 573 K, the acidic OH groups were almost exchanged. All of the observations conclude that O_I and O_{II} are bridging framework oxygen bound to Al (eq 2), the oxygen exchange of O_I and O_{II} with water is promoted by the neighboring proton, and O_{III} is the bridging framework oxygen

TABLE 4: ^{18}O Contents of the Samples Treated in a Large Excess of $H_2{}^{18}O$[a]

zeolite	^{18}O content[b]/% gases water	silanol	acidic OH	Si−O−T	no. of ^{18}O introduced/mmol g^{-1}	unexchanged framework oxygens/mmol g^{-1}
H-MFI-23	93	22 (0.0)	92 (1.2)	10 (3.1)	4.3	29.0
H-MOR-15	90	15 (0.0)	90 (1.7)	19 (6.0)	7.7	25.6
H−FAU-5.6	91	23 (0.0)	87 (3.8)	16 (4.6)	8.4	22.9

[a] Reaction temperature 573 K; reaction time 5 h. [b] Numbers in parentheses are amounts of ^{18}O introduced (mmol g^{-1}). The numbers are calculated on the assumption that the absorption coefficients of ν(silanol) and ν(acidic OH) are equal.

TABLE 5: Changes in ^{18}O Contents for Infrared Bands of Acidic ν(OH) and ν(Si−O−T) with Evacuation at 873 K

zeolite	framework oxygen	^{18}O content/% I[a]	II[b]	I−II[c]/mmol g^{-1}
H-MFI-23	acidic OH	52.3	28.3	−0.32
	Si−O−T	5.6	6.7	0.35
H−FER-17	acidic OH	46.9	30.7	−0.29
	Si−O−T	9.1	10.2	0.37
H-MOR-15	acidic OH	48.0	7.9	−0.78
	Si−O−T	3.5	7.0	1.10
H-LTL-6.0	acidic OH	44.2	11.6	−1.36
	Si−O−T	8.0	12.9	1.43
H−FAU-5.6	acidic OH	51.9	6.6	−1.99
	Si−O−T	3.1	9.2	1.77

[a] In the presence of $H_2{}^{18}O$ at 573 K for 2 h. [b] After the treatment of I, the sample was heated to 873 K with evacuation and evacuated at the same temperature for 1 h. [c] Number of ^{18}O framework oxygens decreased or increased.

between two Si atoms (eq 3). The difference between n_1 and n_2

$$\mathrm{Si}-{}^{16}\mathrm{O}-\mathrm{Al} + \mathrm{H_2}{}^{18}\mathrm{O} \xrightarrow{\text{fast}} \mathrm{Si}-{}^{18}\mathrm{O}-\mathrm{Al} + \mathrm{H_2}{}^{16}\mathrm{O} \quad (2)$$

$$\mathrm{Si}-{}^{16}\mathrm{O}-\mathrm{Si} + \mathrm{H_2}{}^{18}\mathrm{O} \xrightarrow{\text{slow}} \mathrm{Si}-{}^{18}\mathrm{O}-\mathrm{Si} + \mathrm{H_2}{}^{16}\mathrm{O} \quad (3)$$

may result from protruded and shielded Si−O−Al oxide ions, respectively. The conclusion was further supported by the following two findings and two reports. (1) No easily exchanging reaction proceeded on the Na-FAU-5.6 zeolite as shown in Table 3 as has been reported for Na^+- and Ca^{2+}-exchanged stilbite.[31] (2) No easily exchanging oxygen was observed for silica i.e., Si−O−Si framework oxygen: $n_2 = 3.43$; $n_3 = 29.8$ mmol g^{-1}; $k_2 = 80$; $k_3 = 1.1$ min^{-1} mol^{-1}. (3) The Al−O distances are longer in the aluminum tetrahedron compared to the Si−O distances in the silicon tetrahedron.[21,38] (4) Compared to the nonprotonated Si−O−Al bridge, the Si−O and Al−O bonds have become lengthened upon protonation.[21,40] The points of (3) and (4) are consistent with the conclusion that the exchange of bridging framework oxygen bound to Al is fast and promoted by the neighboring proton.

To clarify the change in n_1, n_2, and n_3 at higher reaction temperature, shown in Figure 3a, the H-MFI-23 sample giving the IR spectra of Figure 5b was heated to 873 K with evacuation. The spectrum changed to Figure 5c: The acidic OH bands at 3607 cm^{-1} shifted to higher frequency of 3609 cm^{-1}, while the band for ν(Si−O−T) red-shifted from 1092 to 1091 cm^{-1}. When H-FAU-5.6 was treated in the same way, the spectrum changed from spectrum (b) to (c) in Figure 6: ν(Si−O−T) bands at 1052 cm^{-1} shifted to 1050 cm^{-1}, while acidic OH bands at 3674 and 3596 cm^{-1} shifted to 3688 and 3603 cm^{-1}, respectively. In both cases, the band intensities of OH little changed by the evacuation at 873 K, indicating that the dehydration from the OH species to yield an oxide ion and H_2O did not occur.

The quantitative analysis of infrared spectra is summarized in Table 5. The amount of ^{18}O increase in bridging framework oxygens was 0.35 mmol g^{-1} and approximately agreed with the 0.32 mmol g^{-1} decrease in acidic OH bands in the case of H-MFI-23. Similar agreements between amounts of ^{18}O increased and decreased were observed for H-FAU-5.6 H-FER-17, H-MOR-15, and H-LTL-6.0. These agreements show that the oxygen exchange

$$\mathrm{Si}-{}^{16}\mathrm{O}-\mathrm{Si} + \mathrm{Si}-{}^{18}\mathrm{O}-\mathrm{Al} \rightarrow \mathrm{Si}-{}^{18}\mathrm{O}-\mathrm{Si} + \mathrm{Si}-{}^{16}\mathrm{O}-\mathrm{Al} \quad (4)$$

of O_I and O_{II} with O_{III} proceeds at 873 K as shown in eq 4. Equations 2−4 conclude that the surface acidic OH groups are the gateway to the exchange of the framework oxygen and that the exchange between the framework oxygens becomes easier at higher temperatures.

Acknowledgment. This work was supported in part by a Grant-in-Aid from the Ministry of Education, Science, Sports and Culture of Japan.

References and Notes

(1) Corma, A. *Chem. Rev.* **1995**, *95*, 559−614.
(2) Suib, S. L. *Chem. Rev.* **1993**, *93*, 803−826.
(3) Meier, W. M.; Olson, D. H. *Zeolites* **1992**, *12*, 335−358.
(4) Breck, D. W. *Zeolite Molecular Sieves*; Wiley-Interscience: New York, 1974.
(5) Meriaudeau, P.; Naccache, C. *Catal. Rev.* **1997**, *39*, 5−48.
(6) Zamaraev, K. I.; Thomas, J. M. *Adv. Catal.* **1996**, *41*, 451−654.
(7) Sachtler, W. M. H.; Zhang, Z. *Adv. Catal.* **1993**, *39*, 129−220.
(8) Caro, J.; Bülow, M.; Jobic, H.; Kärger, J.; Zibrowius, B. *Adv. Catal.* **1993**, *39*, 351−414.
(9) Schoonheydt, R. A. *Catal. Rev.* **1993**, *35*, 129−168.
(10) Ono, Y. *Catal. Rev.* **1992**, *34*, 179−226.
(11) Rao, V. J.; Uppili, S. R.; Corbin, D. R.; Schwartz, S.; Lustig, S. R.; Ramamurthy, V. *J. Am. Chem. Soc.* **1998**, *120*, 2480−2481.
(12) Barthomeuf, D. *Catal. Rev.* **1996**, *38*, 521−612.
(13) Haw, J. F.; Xu, T. *Adv. Catal.* **1998**, *42*, 115−180.
(14) Bonn, M.; Bakker, H. J.; Domen, K.; Hirose, C.; Kleyn, A. W.; van Santen, R. A. *Catal. Rev.* **1998**, *40*, 127−173.
(15) Hunger, M. *Solid State Nuclear Magn. Reson.* **1996**, *6*, 1−29.
(16) Farneth, W. E.; Gorte, R. J. *Chem. Rev.* **1995**, *95*, 615−635.
(17) Reinhold: A.; Samoson, A.; Sauer, J.; Bussemer, B.; Lee, Y.; Gann, S.; Shore, J.; Pines, A.; Dupree, R. *J. Am. Chem. Soc.* **1998**, *120*, 3510−3511.
(18) Baba, T. Komatsu, N.; Ono, Y. Sugisawa, H. *J. Phys. Chem.* **1998**, *102*, 804−808.
(19) Mildner, T.; Ernst, H.; Freude, D.; Hölderich, W. F. *J. Am. Chem. Soc.* **1997**, *119*, 4258−4262.
(20) Bates, S. P.; van Santen, R. A. *Adv. Catal.* **1998**, *42*, 1−114.
(21) van Santen, R. A.; Kramer, G. J. *Chem. Rev.* **1995**, *95*, 637−660.
(22) Xu, T.; Barich, D. H.; Goguen, P. W.; Song, W.; Wang, Z.; Nicholas, J. B.; Haw, J. F. *J. Am. Chem. Soc.* **1998**, *120*, 4025−4026.
(23) Stolmar, M.; Roduner, E. *J. Am. Chem. Soc.* **1998**, *120*, 583−584.
(24) Iwamoto, M.; Morita, S.; Kagawa, S. *J. Phys. Chem.* **1981**, *85*, 3995−3957.
(25) Ballmoos, R.; M. Meier, W. *J. Phys. Chem.* **1982**, *86*, 2698−2700.
(26) Takaishi, T.; Endoh, A. *J. Chem. Soc., Faraday Trans. 1* **1987**, *83*, 411−424.
(27) Yamagishi, K.; Namba, S.; Yashima, T. *J. Phys. Chem.* **1991**, *95*, 872−877.
(28) Valyon, J.; Hall, W. K. *J. Catal.* **1993**, *143*, 520−532.
(29) Mori, H.; Mineo, K.; Mizuno, N.; Iwamoto, M. *J. Chem. Soc., Chem. Commun.* **1994**, 975−976.

(30) Mortlock, R. F.; Bell, A. T.; Chakraborty, A. K.; Radke, C. J. *J. Phys. Chem.* **1991**, *95*, 4501−4506.
(31) Xu, Z.; Stebbins, J. F. *Geochim. Cosmochim. Acta* **1998**, *62*, 1803−1809.
(32) Mizuno, N.; Mori, H.; Tajima, M.; Kagawa, S.; Ueno, H.; Yahiro, H.; Iwamoto, M. *J. Mol. Catal.* **1993**, *80*, 229−242.
(33) Iwamoto, M.; Yahiro, H.; Mizuno, N.; Zhang, W.-X.; Mine, Y.; Furukawa, H.; Kagawa, S. *J. Phys. Chem.* **1992**, *96*, 9360−9366.
(34) Kustov, L. M. *Top. Catal.* **1997**, *4*, 131−144.
(35) Zecchina, A.; Bordiga, S.; Spoto, G.; Scarano, D.; Petrini, G.; Buzzoni, R.; Petrini, G. *J. Phys. Chem.* **1996**, *100*, 16584−16599.
(36) Wakabayashi, F.; Kondo, J. N.; Domen, K.; Hirose, C. *J. Phys. Chem.* **1996**, *100*, 1442−1444.
(37) Pelmenschikov, A. G.; van Santen, R. A. *J. Phys. Chem.* **1993**, *97*, 10678−10680.
(38) Czjzek, M.; Jobic, H.; Fitch, A. N.; Vogt, T. *J. Phys. Chem.* **1992**, *96*, 1535−1540.
(39) Flanigen, E. M.; Khatami, H.; Szymanski, H. A. *Adv. Chem. Ser.* **1971**, *101*, 201−229.
(40) Kramer, G. J.; van Santen, R. A. E. *J. Am. Chem. Soc.* **1993**, *115*, 2887−2897.